EFDA–JET–CP(10)05/35

T. Eich, H. Thomsen, W. Fundamenski, G. Arnoux, S. Devaux, A.Herrmann,
S. Jachmich, J. Rapp and JET-EFDA Contributors

ELM Power Deposition Wetted Area and Temporal Shape in JET

ELM Power Deposition Wetted Area and Temporal Shape in JET

T. Eich[1], H. Thomsen[2], W. Fundamenski[3], G. Arnoux[1], S. Devaux[1], A.Herrmann[1], S. Jachmich[4], J. Rapp[5] and JET-EFDA Contributors*

JET-EFDA, Culham Science Centre, OX14 3DB, Abingdon, UK

[1]Max-Planck-Institut fur Plasmaphysik, EURATOM-Association, D-85748 Garching, Germany
[2]Max-Planck-Institut fur Plasmaphysik, EURATOM-Association, D-17XXX Greifswald, Germany
[3]EURATOM-CCFE Fusion Association, Culham Science Centre, OX14 3DB, Abingdon, OXON, UK
** See annex of F. Romanelli et al, "Overview of JET Results",*
(Proc. 22 nd IAEA Fusion Energy Conference, Geneva, Switzerland (2008)).

Preprint of Paper to be submitted for publication in Proceedings of the
19th International Conference on Plasma Surface Interactions, San Diego, California, USA.
(24th May 2010 - 28th May 2010)

ABSTRACT.

A new Infra Red camera (IR) for high resolution infra red studies for the outer divertor target plate in JET has been installed. The temporal resolution of the new system is 86μs and 1.7mm target spatial resolution. Shot integrated energy balance between tile embedded thermo couples and IR based estimation of deposited energy on the outer tile gives fair agreement in the range of 80−120%. The assumptions of the temporal evolution of type-I ELMs power load as made for ITER defines a lower, conservative boundary within the observed variation of the data. The broadening of the ELM induced power profiles are, in contrast to earlier results based on a lower resolution IR system at JET, found to be in the range of 1.4−4 when compared to the inter-ELM wetted area.

1. INTRODUCTION, DATA BASE AND BRIEF REPORT ON DATA VALIDATION

Following the installation of a fast high resolution InfraRed (IR) system viewing the JET divertor a large number of experiments have been performed optimized for power exhaust studies with focus on ELM divertor target power loadings. Type-I ELMy HMode deuterium plasmas with currents from 1MA−3.8MA, q_{95} between 3.3−5.4 and magnetic configurations with low ($\delta = 0.28$) and high ($\delta = 0.4$) triangularity . The measured energy loss from the main plasma for these experiments is in the range of 2−7% normalized to the total plasma thermal energy. This data set with high qualitiy infrared measurements has been analyzed and the results of the analysis compared to the assumptions made for the assessment of the maximum tolerable ELM heat load in ITER. In this paper we present results for the outer divertor only; due to viewing restrictions measurements of the inner divertor are usually of insufficient quality to draw quantitative conclusions. The analysis of the outer divertor measurements presented in this paper is focused on two key issues: (a) the temporal shape of ELM power deposition and (b) the determination of the wetted area for ELM power loading.

The accuracy of the power heat fluxes derived from the IR measurements has been evaluated by cross-checks with other measurements. As an example, Figure 1 shows the energy balance between the shot integrated target energies for the outer divertor from IRbased measurements and thermocouples embedded into the divertor target showing a good agreement between both measurements over a wide set of discharges. With regards to the validation of the power fluxes during the ELMs themselves, Figure 2 shows the comparison of ELM heat fluxes for two otherwise identical discharges where power fluxes have been measured on a CFC tile and a W-coated CFC tile which is located at the same poloidal location and adjacent toroidal position both within the field of view of the IR camera.. The measurements in Figure 2 have been obtained by coherent ELM averaging of 122 ELM events for both discharges. Though the surface IR emissivity and in particular the surface heat transmission coefficient [5] are different for CFC and W, the absolute magnitude of the power fluxes measured on both materials are in remarkably good agreement. This satisfactory comparison increases the level of confidence in the correctness of the evaluation of the absolute magnitude of the ELM induced heat fluxes at the JET divertor on short times scales of ~100μs derived infrared diagnostic providing measurements of the target surface temperature evolution.

Figure 2 also shows a comparison of IR based and Langmuir Probes (LP) based estimation of local heat fluxes at a fixed target position for a coherently averaged ELM representing 99 single events. The target position of the comparison is given by the location of one of the triple probes at JET in the far SOL [10]. The agreement between both systems with respect to the temporal evolution and magnitude of the local heat fluxes is also satisfactory. In addition, the insert in Figure 2 shows a comparison between IR and LP measurements for a single ELM event where single filaments are resolved by both diagnostics. The time difference between the temporal shapes with both diagnostics is found to be in the range of 100us, which is similar to the sampling time of both diagnostics.. However, it can not be ruled out that the time difference between both diagnostics is associated with the physics of energy transport in filamentary structures between the midplane and the divertor and/or the toroidal/poloidal rotation, as both diagnostics are located at different toroidal positions.

2. ELM OUTER TARGET POWER LOAD TEMPORAL SHAPE

Figure 2 shows a typical temporal evolution of the power loading due to type-I ELMs at the JET outer divertor target for a discharge of 2.0MA/2.0T field, no gas puffing $P_{inpu}t$ = 13.5MW by NBI and ELM size of ~6% of the plasma stored energy. Four important parameters can been derived from the temporal shape of ELM power loading to characterize it : a) the rise time and the fall time of the total ELM power load to the divertor. The rise time is defined as the interval in time from the onset of the ELM power pulse to the maximum of the ELM power pulse. The fall time is defined as the interval in time from the maximum of the ELM power pulse to 1/e times this maximum. The rise time in the example in Figure 2 is about 300μs and the fall time 700μs b) The integrated ELM energy deposited at the divertor during both the rise and fall time intervals derived above which are obtained by the time integral of the total divertor ELM power fluxes during these intervals as defined above.

Figure 3 shows the correlation of the rise time with the fall-off time for coherently averaged ELMs from 55 discharges. Each point in this figure corresponds to at least 15 coherently averaged single ELMs events, on average to 100 single ELM events up to more than 300 ELMs for high ELM frequencies. The error bars in this figure represent the statistical scatter of all ELMs within one discharge. The rise time does show a variation of between 200-400μs which is associated, in full accordance with earlier work [3, 8] with the ion transit time defined as the SOL connection length divided by the (ion) sound speed which corresponds to about 220-260μs for ITER [8]. The corresponding fall-off time shows a variation of 500-100μs for a rise time of 250μs. The boundary for which the fall-off time is about twice the rise time defines a lower conservative boundary of the observed data set. Figure 4 shows the ratio of the energy integrated during the fall-off time to that during the rise time for the same 55 discharges. Here, the lower boundary for these measurements is about 2 which is on the upper range of the assumptions taken for ITER. Hence, regarding the temporal shape and integrated energies deposited at the divertor by ELMs the assumptions made for type-I ELM power loadings in ITER to the divertor target are conservative [9]. This conservative approach can be confirmed by comparing the temporal shape of the material tests under ELM-like power fluxes performed for ITER at the TRINITI plasma guns [7] with a typical ELM power flux temporal evolution at the outer JET divertor targert as shown in the insert in Figure 4. The Figure 4 insert shows that the ELM power load evolution absolute time scales for JET and ITER are expected to be nearly identical, since it scales with the connection lengths divided by the ion sound speed [3,8]. The insert also shows that the ELM energy that arrives at the target in long time scales (i.e. after 1ms) can amount to about 30% of the ELM energy flux in JET which is not accounted for by the plasma-gun experiment.

3. ELM POWER LOAD DEPOSITION AREA

The improved instrumental resolution (temporal 86μs/spatial 1.7mm) of the new IR diagnostic at JET has allowed a systematic characterization of the effective area for ELM power deposition (ELM wetted area) and for the power flux between ELMs (inter-ELM wetted area) to be carried out. The wetted area for power flux are defined in simple way be diving the spatially (toroidally and radially) integrated power flux (W) by the peak heat flux (W/m^2). For the inter-ELM power flux, the profiles are averaged in time over a 10 ms time window prior to the ELM event. For ELMs the same method is applied and the values at the peak power flux within ELM power pulse have been taken. Analysis of the database considered in this paper has shown that the wetted area of the inter-ELM power flux profile varies from 0.35m2 to 0.6m2, which corresponds to a mid plane efolding decay length between 4 mm and 7mm and further analysis is on going to determine the physics parameters that determine this variation.

For the comparison of the ELM wetted area versus the inter-ELM area we focus on the results from a gas scan of discharges with current/field of 2.5MA/2.5T (P_{NBI} = 18MW) and another unfuelled discharge at a low current/field of 1.0MA/1.1T (P_{NBI} = 6MW). The ELM target wetted area is found to show a significant broadening in the presence of large ELMs (and a moderate broadening in conditions with smaller ELMs with respect to the inter-ELM wetted area in the same discharges as shown in Figure 5. The change of the ELM size for the 2.5MA/2.5T discharges was achieved by gas puffing. For discharge conditions with large ELMs and lower fuelling the inter-ELM profile is found to be narrower than for high fuelling/smaller ELM discharges. On the contrary, the ELM wetted area scales with ELM energy loss and thus has an opposite trend to the inter-ELM one. This shows that utilizing directly the broadening of the divertor power flux at the ELM compared to the in-between ELMs does not provide a correct physics extrapolation as the divertor power fluxes become broader with decreasing divertor temperature and higher recycling conditions while the ELM power profiles become narrower with decreasing ELM energy loss. The complexity of such comparison is further increased due to the generic filamentary structure of ELM power loadings [1, 2].

As a consequence of the analysis in this paper, a more physics-based extrapolation of the parameters required for the assessment of the material erosion/damage in ITER is proposed. This extrapolation should be based on parameters such as: (a) peak heat flux due to ELMs (W/m^2), integrated ELM energy flux (J/m^2) in the various intervals of the ELM pulse, etc, which will be described in a future paper.. Independently of the outcome of this future analysis., we can conclude that for JET, the typical ELM power profile broadening with respect to inter-ELM power flux profiles is in the range of 1.4 (at low current) to values of about 4 for higher current discharges in absence of gas puffing.

CONCLUSIONS

The main conclusion to be drawn from the analysis of the characteristics of ELM power loading reported in this paper, besides the increasing levels of confidence on the IRbased heat flux estimation for ELMs, is that the ELM wetted area is not a constant fraction of the inter-ELM wetted area of the order of one as reported earlier [3], but does depend on the magnitude of the ELM energy loss or ELM size. For smaller ELMs, at fixed field/current of 2.5MA/2.5T obtained by gas puffing, a significantly smaller ELM wetted area than for larger ELMs is found. It is found that the ELM wetted area increases linearly with ELM size and a broadening of up to 4 is found for the largest ELMs in the database analysed. This JET result is in line with recent data published from DIII-D IR analysis for the inner target [6]. For very small ELMs at low current a small broadening of ~ 1.4 is found at JET which is in agreement with the low values of broadening reported for ASDEX Upgrade for discharges with plasma current of 0.8-1MA [4]. Future work will concentrate on the scaling of the ELM wetted area and power/energy fluxes with physics based parameters such as pedestal parameters, ELM energy loss, etc., which might be a challenging task in the presence of ELM filaments and their intrinsic toroidal asymmetries that need to be incorporated into a 1-d power profile [2,1]. However, the reported effect of ELM wetted area broadening, although only measured for the outer target at JET,, may allow a revision of the conservative specifications for uncontrolled ELMs in ITER for which a ELM power profile broadening of one is assumed. On the contrary, it is not clear if the findings in this paper may lead to a revision of the ITER assumptions for controlled ELMs as the broadening in this case is expected to be one.

The time scales fro ELM power deposition in this analysis, as reported earlier [3, 4], confirm that the current assumptions for the temporal shape of the ELM power load shape in ITER define a lower boundary of the actual observed data. Also here, a possible slight relaxation of the minimum ELM size for ITER by about 30-50% may be possible. Providing an accurate estimate for this requires dedicated modeling and testing as this estimate depends on the material properties themselves.

REFERENCES:

[1]. Devaux S. et al., this conference

[2]. Eich T. et al., Physical Review Letter **91**, 195003 (2003)

[3]. Eich T. et al., Journal of Nuclear Materials, **337-339**, p. 669 (2005)

[4]. Herrmann A. et al, Journal of Nuclear Materials, **313-316**, p.759 (2003)

[5]. Herrmann A. et al, Physics Scripta, T**128** (2007)

[6]. Jakubowski M. et al., Nuclear Fusion **49**, 095013 (2009)
[7]. Klimov, et al., Journal of Nuclear Materials **390** 391 (2009) p. 721.
[8]. Loarte A. et al., Plasma Physics and Controlled Fusion, **45** (2003), p.1549
[9]. Loarte A., private comm., ITER Plasma Performance Assessment (ITER_D_22HGQ7).
[10]. Tshkakaya D. et al., this conference

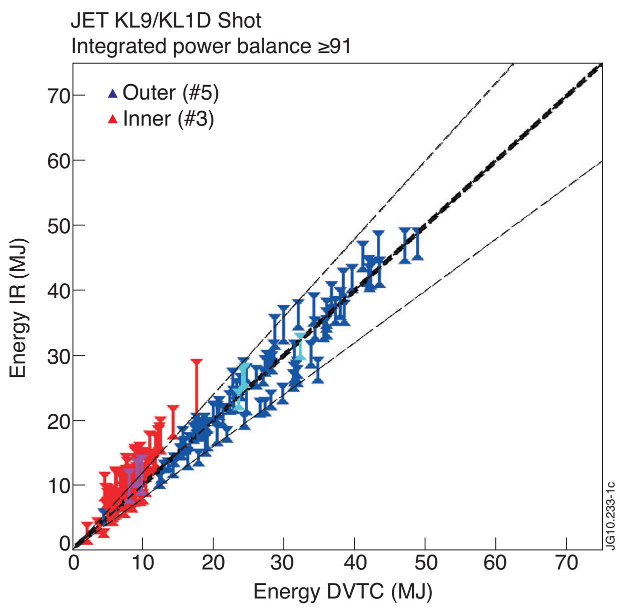

Figure 1: Comparison of IR and thermocouple (DVTC) derived energies for 91 discharges for outer (blue) and inner (red) divertor tiles. Integration time is the entire pulse duration (~10sec.)

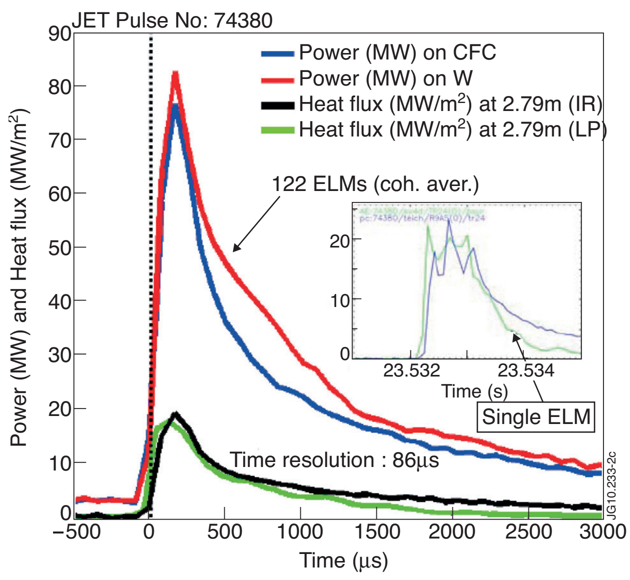

Figure 2: Comparison of derived power fluxes for CFC and W coated tiles from IR from two identical discharges (Pulse No's: 74380 + 74384) during a coherently averaged ELM, complemented by a comparison of local heat flux from IR and Langmuir probes for the same discharge (Pulse No: 74380), again for a coherently averaged ELM representing 99 events.

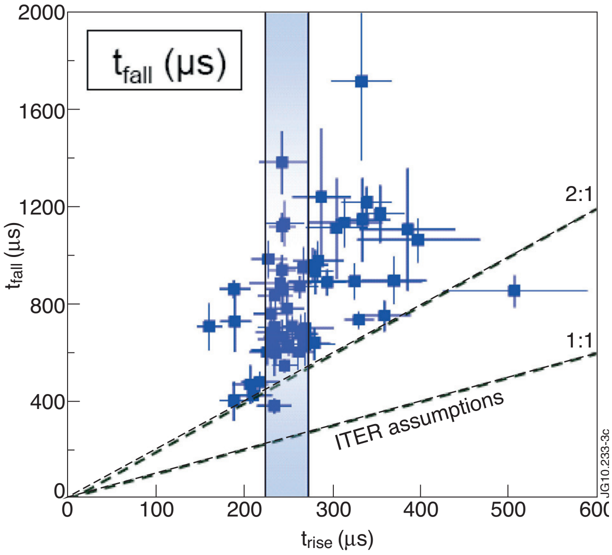

Figure 3: Comparison of the fall time to the rise time of the temporal power load shape during type-I ELMs. The upper range of the assumptions ITER assumptions that that fall times is 1-2 the rise time defines a lower conservative boundary

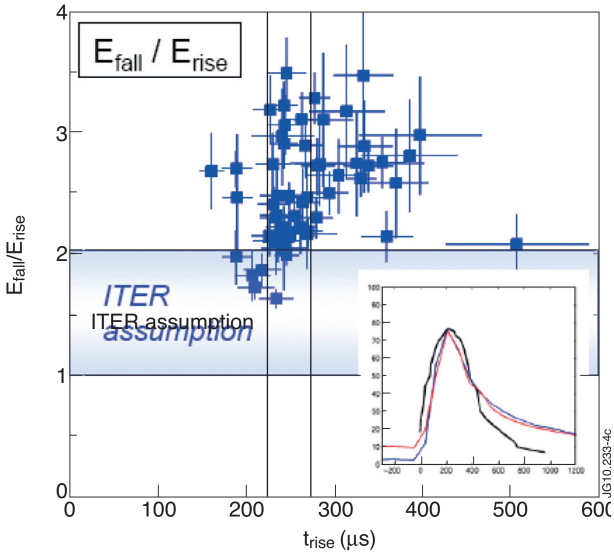

Figure 4: The ratio between the energy integrated during the rise time to the energy during the fall time (1/e criterion after the peak heat flux). The insert shows the comparison of a coherently averaged ELM (Pulse No: 79745, ~100 ELMs) for (blue) power flux and (red) peak heat flux to the temporal shape as used by the TRINIT plasma gun (normalised to match the peak).

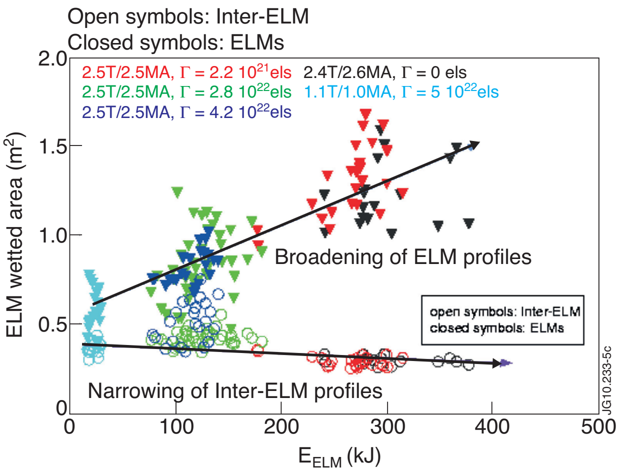

Figure 5: Effective wetted area during an ELM event and prior to the ELM event. The wetted area is calculated by dividing the tile integrated power flux (MW) by the maximum local heat flux (MW/m^2). For small ELMs very little broadening is observed (1.4) and for large ELMs a significant broadening of about 4.